Theor Chim Acta (1992) 81: 303–318

Theoretica Chimica Acta

Proton transfer in the water dimer catalyzed by doubly charged cations (Zn^{+2}, Be^{+2}, and Mg^{+2})

An *ab initio* study*

Miquel Solà, Agustí Lledós, Miquel Duran, and Juan Bertrán
Departament de Química, Universitat Autònoma de Barcelona, 08193 Bellaterra, Catalonia, Spain

Received December 20, 1990/Accepted April 1, 1991

Summary. The proton transfer process in the water dimer complex catalyzed by three divalent metal ions has been studied through *ab initio* methods using different basis sets. Calculations with a dipositive charge placed at different distances from one of the oxygens of the water dimer have been also performed. A catalysis found in this process owing to both electrostatic and charge-transfer effects. Morokuma analyses show that the electrostatic effect is the most important for this proton transfer. The effect of the ligands in the coordination sphere of Zn^{+2} is also discussed by studying the same proton transfer process in a Zn^{+2} complex with three NH_3 ligands.

Key words: Proton transfer – Water dimer – Dications – Ligands

1. Introduction

The importance of the proton transfer in many biochemical and catalytic processes is well established [1]. One of the most elementary proton transfers that can be considered takes place in the water dimer yielding the hydroxyl and the hydronium ions. This process in the gas phase is very unfavoured; on the contrary, it is known that this process occurs easily in many biochemical systems where dications are present in the active site of the metalloenzyme [2]. Therefore, one might conclude that dications should catalyze the proton transfer in the water dimer.

A general scheme for the proton transfer between the AH and B species can be written according to:

$$\underset{\text{R}}{A-H+B} \rightarrow \underset{\text{RC}}{A-H\cdots B} \rightarrow \underset{\text{TS}}{AHB} \rightarrow \underset{\text{PC}}{A^-\cdots H^+-B} \rightarrow \underset{\text{P}}{A^-+HB^+} \qquad (1)$$

where R, RC, TS, RP and P stand for reactants, reactant complex, transition state, product complex and products, respectively.

* A contribution from the "Grup de Química Quàntica de l'Institut d'Estudis Catalans"

For the isolated water dimer, scheme (1) presents an RC, although neither a TS nor a PC are found. In this case, the energy increases continuously from the initial RC to the final separated ions. When a Li^+ ion is incorporated to this system, it has been shown that even though the energy profile is stabilized everywhere, no PC appears at all [3]. If the Li^+ ion is substituted by a proton, the $H(H_2O)_2^+$ system is formed. In this species, the proton transfer has been shown theoretically to have a U-shaped symmetric energy profile [4]. Here, only one symmetric complex where the proton is halfway transferred between the two oxygens is found.

To our knowledge no one has studied the influence of a dication on the water dimer, although some studies have appeared dealing with the influence of dications on the proton transfer in other dimers. In particular, Basch et al. [5] studied the proton transfer in the imidazole dimer under the influence of a Zn^{+2} cation. These authors found that in the isolated imidazole dimer the RC was more stabilized than the PC, whereas in the presence of a Zn^{+2}, the PC became more stabilized than the RC, leading to a substantial decrease in the energy barrier.

The purpose of the present work is to carry out a comparative study of the role played by different dications on the proton transfer in the water dimer. In particular, we will focus on the Zn^{+2} cation, which has been shown to play a catalytic role in some similar processes. In addition, from an experimental point of view this cation plays an important role in many biochemical processes. For instance, the Zn^{+2}–(OH^-) species generated from a Zn^{+2}-bound water has been suggested to be the active species in several enzymatic reactions [2]. The results for Zn^{+2} will be compared with those of Be^{+2}, Mg^{+2} and the more general case of a dipositive charge, which will allow one to get a deeper insight into the specificity of zinc in this kind of processes. Experimentally, Zn^{+2} never acts as a naked dication in enzymes. On the contrary, it is found usually coordinated to four ligands. For instance, in the carbonic anhydrase enzyme the Zn^{+2} ion is coordinated to three imidazole groups and one water molecule forming a slightly distorted tetrahedrical geometry [2a, 2b, 2d]. Thus, to get a more realistic description of the proton transfer in the water dimer, the effect of ligands has been also considered by coordinating a Zn^{+2} cation to three NH_3 ligands.

2. Method

Ab initio SCF calculations were carried out using the Hartree–Fock–Roothaan method [6]. Full geometry optimizations of minima were performed by means of the Schlegel [7] and Broyden–Fletcher–Goldfarb–Shanno [8] algorithms. Transition state structures were directly located using Schlegel's method [7]. Minima and transition states were characterized by the correct number of negative eigenvalues of their Hessian matrices.

It is well known that the quantitative description of proton transfers in charged systems requires the use of large basis sets which include polarization and diffuse functions; furthermore, correlation energy and zero-point corrections must be accounted for [1b, 4, 9]. If the size of the chemical system being studied prevents use of such high level of theory, it has been shown that the minimum level of theory for which semiquantitative results can be obtained involves a double-ζ plus polarization basis set. Moreover, for anions diffuse functions must be added [10]. In the present study on cationic systems, one of the chemical

species involves Zn. Thus, to accomplish the aforementioned minimum level of theory we have used a (33321/3321/21/1) basis set for Zn, which means a double-ζ set for the highest *s*, *p* and *d* orbitals, together with a polarization *f* function. This basis set has been built starting from the 3-21G basis set [11], which has been recently extended to third-row atoms. This set has been supplemented by an *f* function with an exponent of 1.3375 [12]. This same level has been represented for the other atoms (Be, Mg, O) by means of the 3-21G basis set supplemented with *d* functions ($\alpha_{Be} = 0.4000$ [13], $\alpha_{Mg} = 0.1750$, $\alpha_O = 0.8000$ and $\alpha_N = 0.8000$ [13]). For identification purposes, we label this basis set 3-21G(d, f). To discuss the importance of including polarization functions and splitting the valence functions, calculations with smaller basis set have been carried out as well. First, we have employed the MINI-3 minimum basis set [14], which has no valence *p* basis functions for Be, Mg and Zn; second, we have made use of the split-valence 3-21G basis set; and finally, we have performed valence-only calculations. In this case, the effective-core-potentials (ECP) given by Hay and Wadt [15] for Zn and Mg, the valence basis set [3*s*, 2*p*, 5*d*/1*s*, 1*p*, 2*d*] for Zn, [3*s*, 3*p*/1*s*, 1*p*] for Mg, and the 4-31G basis set [16] for hydrogen and oxygen.

When three ammonia ligands have been included in the calculations, the optimizations have been performed using the 3-21G basis set for all atoms. However, the hydrogens of the ammonia groups have been represented through the STO-3G basis set. We will label this mixed basis set as '3-21G'. In these calculations, the N–H distance has been kept frozen to 1.050 Å and the $\widehat{NHN}$ angle to 109.407°. Furthermore, we have recalculated the energies for these 3-21G optimized structures using the 3-21G(d, f) basis set. We have labelled this level of calculation as 3-21G(d, f)//3-21G.

All calculations presented in this paper were carried out with the help of the GAUSSIAN 86 [17] and MONSTERGAUSS [18] programs.

3. Results and discussion

As mentioned in the Introduction, the goal of this paper is to study the proton transfer in the $M^{+2}(H_2O)_2$ system (M = Zn, Be and Mg). The results obtained are split into four sections: first, the results for the proton transfer in the $M^{+2}(H_2O)_2$ system are presented; second, the catalytic role of the cation is analyzed; third, a methodological discussion is performed; and finally, the effects of the ligands are considered.

3.1. Proton transfer in the $M^{+2}(H_2O)_2$ systems

This section presents the study of the proton transfer reaction. For each metal cation we have located an intermediate and a transition state. Therefore, the structures of these species are presented first, and later the energy profiles are discussed. All results are obtained through use of the 3-21G(d, f) basis set.

Intermediates. For the intermediates, Table 1 collects the distance from the metal to the oxygen, distances from the oxygens to the transferring proton, Pauling bond orders for these O–H bonds, and charges on the metal and the H_3O fragment. Values obtained for $H(H_2O)_2^+$ and the isolated water dimer systems

Table 1. Distances from O_1 to the metal, distances from oxygens to the transferring hydrogen and their corresponding Pauling bond orders (B), and charges on the metal (q_M) and H_3O fragment ($q_{(H_3O)}$) for the $M^{+2}(H_2O)_2$ species obtained through use of the 3-21G(d, f) basis set. The values corresponding to the $H(H_2O)_2^+$ and water dimer intermediates are also given. Distances are given in Å, and charges in atomic units

Ion	$r(MO_1)$	$r(O_1H_1)$	$r(O_2H_1)$	$B^a(O_1H_1)$	$B^a(O_2H_1)$	q_M	$q_{(H_3O)}$
Zn^{+2}	1.732	1.447	1.060	0.199	0.784	1.568	0.869
Be^{+2}	1.404	1.942	0.995	0.001	0.975	1.275	0.939
Mg^{+2}	1.803	1.346	1.108	0.279	0.668	1.556	0.834
H^+	0.969	1.194	1.194	0.463[a]	0.502[a]	0.523	0.800
—	—	0.967	1.894	0.987	0.049	—	—

[a] Pauling bond orders were calculated through the expression $B = \exp\{[R(1) - R(B)]/0.3\}$. The bond order for O_1-H_1 is referred to the O–H distance in water ($R(1) = 0.964$ Å) and the O_2-H_1 is referred to the O–H distance in the hydronium ion ($R(1) = 0.987$ Å)

are also included for comparison purposes. Finally, the geometries of the $M^{+2}(H_2O)_2$ (M = Zn, Be, and Mg) species are depicted in Fig. 1.

The optimal 3-21G(d, f) geometry of the $H(H_2O)_2^+$ species exhibits a linear symmetric hydrogen bond where the proton is located midway between the two oxygen atoms. This structure belongs to the D_{2d} symmetry point group, with the planes of the two water molecules staggered by 90 degrees with respect to one another. The structure of this species is strongly dependent on the basis set and the level of calculation employed. Previous very good calculations yielded a symmetrically hydrogen-bonded proton [4d, b]. When the hydrogen is substituted by dications, the geometry of the minimum changes and symmetry is destroyed, as one can see from the values of the distances between the two oxygens and the transferring hydrogen in Table 1. The intermediates found for the $H(H_2O)_2^+$ system and for the $M^{+2}(H_2O)_2$ systems exhibit a different nature. Whereas in the first case the proton is halfway transferred, in the $M^{+2}(H_2O)_2$ systems the proton transfer is already done and the H_3O^+ species has been formed. Starting from the O_1-H_1 distances and the bond orders, one can see that for Zn^{+2} and Mg^{+2} some amount of bonding character is left between the O_1 and H_1 atoms. On the contrary, for the Be^{+2} complex this bond is broken. This aspect is related to the fact that the distance between Be and O_1 is the shortest one among these intermediates.

In order to relate the studied proton transfer to scheme (1) it is necessary to split the $M^{+2}(H_2O)_2$ system into $M^{+2}H_2O$ and H_2O. Keeping in mind this

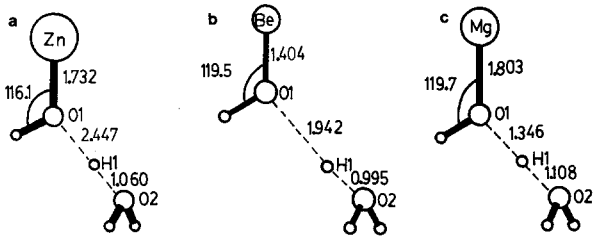

Fig. 1. Optimized structures of the hydrogen bond complexes computed with the 3-21G(d, f) basis set: (**a**) $Zn^{+2}(H_2O)_2$; (**b**) $Be^{+2}(H_2O)_2$; (**c**) $Mg^{+2}(H_2O)_2$

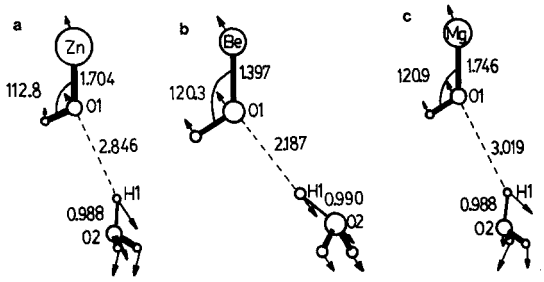

Fig. 2. Optimized structures of the transition states of the proton transfer processes computed with the 3-21G(d, f) basis set: (**a**) $Zn^{+2}(H_2O)_2$; (**b**) $Be^{+2}(H_2O)_2$; (**c**) $Mg^{+2}(H_2O)_2$

scheme, the intermediate should correspond to the PC species. Further, neither a RC nor a TS should exist in the proton transfer in $M^{+2}(H_2O)_2$ species. By looking at the charge on the H_3O group in Table 1, it can be seen that the proton transfer in the $M^{+2}(H_2O)_2$ systems is more advanced for the Be^{+2} complex. The values of the charge on the metal show some amount of correlation between the electron-withdrawing capacity of the metal and the degree of advance in the proton transfer reaction.

Transition states. For all systems studied, a transition state is found because products are stabilized, in contrast to the $H(H_2O)_2^+$ system. Transition state geometries and transition vectors are depicted in Fig. 2. Energy barriers, geometries, charges on the metal and on the H_3O fragment are shown in Table 2.

When one compares the geometries of the transition states with those found for the intermediates it can be seen that the H_3O^+ ion formed is placed far away from the MOH^+ species. The most striking fact is that the shorter the distance in the transition state is, the longer it is in the intermediate. The bond orders in the forming and breaking bonds, together with the charges on the H_3O fragment, bring about similar conclusions.

Another appealing aspect is that the $M-O_1$ distances have shortened when going from the intermediate to the transition state, in connection with the fact that a more important charge transfer takes place in the transition state, as confirmed by the values of the charge on the metal in Tables 1 and 2.

The eigenvectors associated to the only negative eigenvalue of the Hessian matrices (depicted in Fig. 2) indicate that these transition states do not really correspond to the proton transfer process, but rather to the separation between two charged species (MOH^+ and H_3O^+).

Table 2. Energy barriers of the proton transfer referred to intermediates, distance from metal to O_1, distances to the oxygens from the transferring hydrogen, and charges on the metal and the H_3O fragment for the transition states, computed with the 3-21G(d, f) basis set. Energies are given in kcal/mol, distances in Å, and charges in atomic units

Ion	ΔE	$r(MO_1)$	$r(O_1H_1)$	$r(O_2H_1)$	q_M	$q_{(H_3O)}$
Zn^{+2}	9.5	1.704	2.846	0.988	1.433	0.993
Be^{+2}	0.1	1.397	2.187	0.990	1.252	0.960
Mg^{+2}	14.0	1.746	3.019	0.988	1.405	0.995

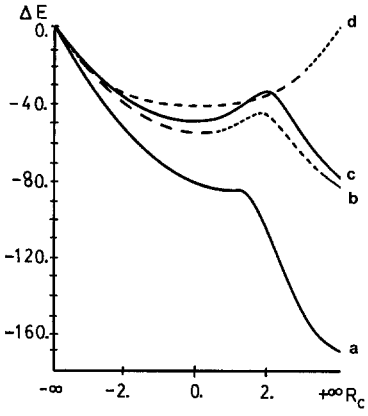

Fig. 3. Energy profiles for the three $M^{+2}(H_2O)_2$ systems and for $H(H_2O)_2^+$ computed with the 3-21G(d, f) basis set: (**a**) M = Be; (**b**) M = Zn; (**c**) M = Mg; (**d**) M = H. R_c in Å and ΔE in kcal/mol

Energy profiles. The energy profiles for the proton transfer reactions are given in Fig. 3. The reaction coordinate R_c is chosen as the difference between the O_1-H_1 and O_2-H_1 distances. As mentioned above, when going from the intermediate to the transition state, the metal-oxygen distance decreases along the reaction coordinate, so it is important to optimize it. Otherwise the energy barrier would increase and the electron transfer would be smaller. In Fig. 3, the energies are referred to the system $M^{+2}H_2O + H_2O$, for which the reaction coordinate (R_c) has a value of $-\infty$, whereas for the final products MOH^+ and H_3O^+ $R_c = \infty$. If the energy were referred to the metal dications and the water dimer, the energies for the intermediate would be -160.0, -235.1, and -137.7 kcal/mol, for Zn^{+2}, Be^{+2}, and Mg^{+2}, respectively.

From Fig. 3 it emerges clearly that the symmetric shape of the $H(H_2O)_2^+$ system disappears for the metal systems. The curves for Mg^{+2} and Zn^{+2} follow a similar trend to the $H(H_2O)_2^+$ curve from reactants until the transition state. In contrast, the curve is fairly different for Be^{+2}. The values of R_c in the intermediate, which is 0.000 for the $H(H_2O)_2^+$ system, are 0.387, 0.947 and 0.238 for Zn, Be, and Mg, respectively. As pointed out in the preceding section, the transition state for Mg^{+2} is more advanced than that found for Zn^{+2}, and this one is in turn more advanced than that obtained for Be^{+2}. This can be explained by looking at Fig. 3, where it is shown that the transition states are more advanced in the reaction coordinate the less exothermic the reaction is, in complete agreement with Hammond's principle. Several differences arise when one compares the energy profiles obtained for the three dications with the more general double-well profile of the proton transfer processes represented by scheme (1). First, as mentioned previously, neither RC nor TS for the proton transfer appear. Second, the overall process is highly exothermic, with a TS which corresponds to the separation between two charged species (H_3O^+ and MOH^+).

The similarity between the Mg^{+2} and Zn^{+2} profiles suggests that the $3d^{10}$ filled orbitals of the Zn^{+2} do not intervene in the proton transfer process. In addition, the $3d$ Mulliken population values at different points along the reaction coordinate remain almost constant during the reaction. Nevertheless, small changes are observed for the d_z^2 Mulliken population. It has been previously observed [19] that the $3d$ electrons of Zn belong really to the core and have minimal interactions with the other orbitals. This point will be discussed later on.

The charge transfer to the metal during the reaction goes to the empty *s* and *p* orbitals of the zinc. The same trend is observed for beryllium and magnesium.

3.2. Catalytic role of the cation

The proton transfer in the isolated water dimer is very difficult due to two main reasons: first, the formation of the OH^- and H_3O^+ ions; second, their separation. For instance, 3-21G(d, f) calculations yield 284 kcal/mol as the difference between the infinitely-separated ions and the water dimer. In contrast, the proton transfer process is favoured if a monovalent ion catalyzes the reaction [3, 20]. In this case, there is no longer a charge separation, but rather a migration of the positive charge, which is not so unfavoured energetically. The separation between the created dipole and a positive charge is not so difficult as the separation in the non-catalyzed processes, where two opposite charges must be pulled apart. In particular, if the monovalent ion is a proton, the difference between the infinitely-separated products (H_2O and H_3O^+) and the intermediate is 41 kcal/mol. If the proton transfer is catalyzed by a dication, the process is further favoured, which can be attributed to two main reasons. First, the positive charge is spread over two fragments, and second, the appearance of a positive charge in each fragment helps the separation towards the final products. This fact translates into the exothermicity of the proton transfer catalyzed by the three cations considered in the present work.

The catalytic effect of divalent metal ions on the proton transfer in the water dimer can be seen to be caused by two main reasons: an electrostatic effect and a charge transfer effect. In order to separate these two factors, we have simulated the cations by a dipositive charge placed at different distances from the oxygen atom (1.9, 1.6 and 1.4 Å). In this way, it is possible to study the purely electrostatic effect. The presence of the dipositive charge causes an important polarization of the electronic cloud of the water dimer. In Fig. 4, the difference in electron density between the water dimer and the same structure with a dipositive charge placed at 1.4 Å from the O_1 atom is presented. One can observe an increase in electron density around the O_1 and a decrease in the adjacent hydrogens. In the fragment that will be the final hydroxyl group, the charge has been changed by effect of polarization from -0.479 to -0.693 when a dipositive

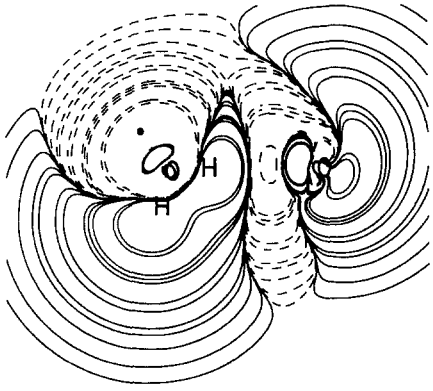

Fig. 4. Plot of electron density differences for the 3-21G(d, f) basis set, between the optimized water dimer and the same structure when a dipositive charge has been placed at 1.4 Å. Negative values are represented through dashed lines and positive values through continuous lines. • indicates the site of the dipositive charge

Table 3. Forces acting on the two O–H bonds and their Mulliken indexes in the dipositive charge-water dimer complex computed with the 3-21G(d, f) basis set. The charge is placed at a distance d from oxygen. Distances are given in Å, and forces and Mulliken indexes in atomic units

d	$F(O_1H_1)$	$F(O_2H_1)$	$P(O_1H_1)$	$P(O_2H_1)$
∞	0.0000	0.0000	0.2459	0.0506
1.9	0.0199	−0.0141	0.1999	0.0877
1.6	0.0313	−0.0197	0.1749	0.0967
1.4	0.0437	−0.0249	0.1484	0.1045

charge has been located at 1.4 Å. Therefore, as a first consequence of polarization, separation into a positive and a negative charge is more advanced. As a second consequence, a weakening of the O_1-H_1 bond and a strengthening of the hydrogen bond (O_2-H_1) is produced, as can be seen from the values of the Mulliken populations in Table 3. The changes in bond strength are larger the closer to the oxygen atom the charge is placed. In Table 3 we have also collected the gradients acting on the two considered O–H distances. For the optimized isolated water dimer, gradients are indeed zero. In contrast, when the positive charge is placed close to oxygen, forces appear trying to lengthen the O_1-H_1 bond and to shorten the hydrogen bond. The origin of such forces can be found in the attraction between the negative oxygens and the positive charge, and the repulsion between the positive charge and the transferring proton. These forces are larger the shorter the charge-oxygen distance is, and help the water dimer to relax, so the optimized geometries of the charge-water dimer complex are modified. For the aforementioned three values of the charge-oxygen distance, the energy profiles for the proton transfer process were obtained, and minima and transition states were located in the full potential energy surface. The results obtained are collected in Table 4, and depicted in Fig. 5.

Table 4. Stabilization energies of minima referred to separated reactants (H_2O^{+2} and H_2O), and energy barriers of transition states referred to intermediates, distances from the oxygens to the transferring hydrogen, and charges on the H_3O fragment, for the systems where dipositive charges are placed at different distances from the $(H_2O)_2$ dimer, computed with the 3-21G(d, f) basis set. Relative energies are given in kcal/mol, distances in Å, and charges in atomic units

Distance	Species	ΔE	$r(O_1H_1)$	$r(O_2H_1)$	$q_{(H_3O)}$
1.9	Minimum	−38.9	1.032	1.481	0.677
	TS	56.0	3.743	0.982	1.000
1.6	Minimum	−50.0	1.178	1.230	0.788
	TS	28.3	3.323	0.982	0.998
1.4	Minimum	−68.1	1.473	1.047	0.886
	TS	14.0	3.007	0.982	0.995

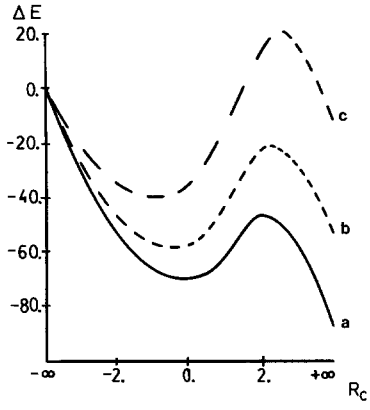

Fig. 5. Energy profiles for the dipositive charge-$(H_2O)_2$ complexes for different charge-oxygen distances (d) computed with the 3-21G(d, f) basis set: (**a**) $d = 1.4$ Å; (**b**) $d = 1.6$ Å; (**c**) $d = 1.9$ Å. R_c in Å and ΔE in kcal/mol

Looking at this figure, one can see that the energy profiles are qualitatively similar to those for the systems with the metal dications, although the transition states for the dipositive charge are found later along the reaction coordinate. The difference in behaviour between Zn, Be, and Mg can already be explained by inspection of the metal-oxygen distances for the intermediate in Table 1, which are initially 1.732, 1.404 and 1.803 Å respectively. This qualitative agreement is not at all quantitative. For instance, a dipositive charge must be placed at 1.4 Å so that the energy profile is similar to that of the Mg^{+2}-catalyzed profile, where the initial Mg–O distance in the intermediate is *ca.* 0.4 Å longer. This fact can also be observed from the charges on the H_3O fragment and the geometries of the intermediates and the transition states, showing clearly that to interpret the proton transfer process the electrostatic effect is not the only cause to be considered, so the charge transfer effect must also be taken into account. The divalent metal does not only act like a dipositive charge, but like a Lewis acid as well. This behaviour is produced by accepting electronic charge into the empty orbitals of the metal. As mentioned above, in Zn d orbitals make almost no intervention, so in all three metals only s and p orbitals are ready to accept charge. The proton transfer reaction will proceed more easily when the s and p orbitals of the metal are closer to the donor orbitals of the $(H_2O)_2$ complex. Thus, the observed difference between the three metals can also be related to the energies of the s and p metal dication orbitals, which are collected in Table 5.

Table 5. Energies of the s, p, and d valence orbitals for the metal dications (in eV) computed with the 3-21G(d, f) basis set

Ion	Orbital	Energy
Zn^{+2}	4*p*	−10.63
	4*s*	−15.74
	3*d*	−37.19
Be^{+2}	2*p*	−14.02
	2*s*	−17.95
Mg^{+2}	3*p*	−10.40
	3*s*	−14.61

For Zn^{+2} the energies of these orbitals are found to lie between those of the Be^{+2} and Mg^{+2} orbitals, yet closer to the Mg^{+2} energies. Thus, the different behaviour as Lewis acids helps to explain the different results found in the present study for the three metals. Their behaviour is originated both by an electrostatic effect and by their Lewis acid character.

In order to have a more quantitative idea of the weights of electrostatic and charge transfer contributions, a decomposition of the interaction energy of the intermediates by means of a Morokuma energy decomposition analysis [21] has been performed. The two fragments considered have been the naked dication and the water dimer. In Table 6 the results obtained through this analysis are reported. The stabilization energy (ΔE) is decomposed into two terms. The first one is the geometrical deformation of the water dimer in the intermediates (ΔE_{def}), and the second one corresponds to the interaction between the deformed water dimer and the dication (ΔE_{INT}). The latter has been decomposed into five terms, namely, electrostatic (ES), polarization (PL), exchange (EX), charge transfer (CT), and mix (MIX) terms. In Table 6 the interaction energy when a dication has been substituted by a dipositive charge (ΔE_{dic}) is also reported.

Although the electrostatic plus polarization (ES + PL) and the charge transfer (CT) terms order the dications in the same way, it is worth noting that the ES + PL term is much more important than the CT term, both from the absolute energy value of these terms for each cation, and from the relative energy differences between the values corresponding to each cation within a given term.

The EX term decreases when going from Be^{+2} to Mg^{+2} due to the increase in the metal-oxygen distance, as one can expect. On the contrary, this term increases for Zn^{+2} remarkedly even though the Zn–O and Mg–O distances are of the same order. This fact must be attributed to the electron repulsion created by the filled $3d^{10}$ orbitals of Zn. Another special behaviour presented by Zn^{+2} can be seen when one compares the ES + PL term with the ΔE_{dic} for the three studied dications. The difference between these two terms should give a first approximation to the polarization made by the charge distribution of the water dimer on the electronic cloud of the dication. Whereas for Be^{+2} and Mg^{+2} this difference leads to an additional stabilization of *ca.* 6 kcal/mol, for Zn^{+2} this difference is *ca.* 30 kcal/mol, so a more remarkable effect is found for Zn^{+2} owing to the easier polarization of the *d* shell. These results indicate that the simulation of a dication by a dipositive charge is acceptable in the case of Be^{+2} and Mg^{+2}, where the polarization of the dication by the water dimer is negligible, although it is a more rough approximation for the Zn^{+2} dication.

From the results presented in Table 6 one can compare the effects of the studied dications. The Be^{+2} ion is the most different according to either the ES

Table 6. Morokuma energy decomposition analysis including correction of the BSSE, for the intermediates. The two fragments considered are the naked ion and the water dimer. Energies are given in kcal/mol

	ΔE	ΔE_{def}	ΔE_{INT}	ES	PL	EX	CT	MIX	ES + PL	ΔE_{dic}
$Zn^{+2}(OH_2)_2$	−160.0	67.1	−227.8	−181.3	−60.2	65.4	−33.3	−17.8	−241.5	−211.8
$Be^{+2}(OH_2)_2$	−235.1	112.3	−347.4	−249.5	−118.2	58.0	−55.0	17.3	−367.7	−361.3
$Mg^{+2}(OH_2)_2$	−137.7	55.2	−192.8	−148.3	−44.4	20.4	−28.9	−0.7	−192.7	−186.7

or CT terms. Furthermore, it has been pointed out in the preceding section that Mg^{+2} and Zn^{+2} have a more similar behaviour. From the values of Table 6 it arises clearly that this similarity is accomplished through compensation by the different terms implied. In fact, the filled $3d^{10}$ shell gives some particularities to the zinc dication. On one hand, these $3d^{10}$ orbitals place the empty $4s$ and $4p$ orbitals in the adequate level for the optimal catalysis of the proton transfer. On the other hand, the $3d^{10}$ shell increases the EX term noticeably. Finally, in spite of its fixed occupation, there is an important polarization effect which must be taken into account.

3.3. Methodological considerations

The results discussed above were obtained with the 3-21G(d, f) basis set. Among the basis sets used, this is the only one that incorporates polarization functions, which has been shown to be essential in the semiquantitative description of similar proton transfer processes [1a, 4, 10]. To test the different basis sets used the proton transfer in the $H(H_2O)_2^+$ systems, for which experimental values are available, has been studied. In Table 7 we report the values of the stabilization energy of the $H(H_2O)_2^+$ system relative to isolated H_3O^+ and H_2O obtained with different basis sets together with the experimental value. It can be seen that the 3-21G(d, f) value is the closest one to the experimental result among the basis sets used, showing the reliability of this basis set. In addition, among the basis sets used, it is the only one that reproduces the pyramidal geometry of the H_3O^+ species predicted theoretically with larger basis sets [22]. As can be seen in Table 7 the MP2/6-311 + G(2d, 2p) basis set gives the best energy result [9], although the use of such basis sets in systems which incorporate transition metals is impractical due to computational limitations.

Table 8 reports the geometry of the intermediates, the stabilization energies from $M^{+2}OH_2$ and H_2O and the energy barrier referred to intermediates with each dication and for all basis sets used. The first remarkable fact is the strong sensitivity of the results with respect to the basis set used. Further, one can see that in all the studied cases, the proton is already transferred in the intermediates with the 3-21G(d, f) basis set. In the same way, whenever pseudopotentials are used (Zn and Mg dications) the proton is also transferred. With the 3-21G basis set the proton transfer is finished for the Zn and Be dications, although it has not been carried out yet for the Mg dication. Finally, MINI-3 basis set results show in all cases that the proton is not yet transferred.

Table 7. Stabilization energies for the $H(H_2O)_2^+$ system from H_3O^+ and H_2O in kcal/mol

Basis set	ΔE
3-21G(d, f)	40.1
3-21G	52.6
Pseudop.	43.9
MINI-3	51.5
MP2/6-311 + G(2p, 2d)	34.0[a]
Exp.	31.6–36[b]

[a] From Ref. [9]
[b] From Ref. [23]

Table 8. Stabilization energies of minima (ΔE_s) referred to separated reactants, and energy barriers of transition states ($\Delta E^{\ddagger}$) referred to intermediates, and distances from the oxygens to the transferring hydrogen at the geometry of the intermediates computed with the different basis set used. Relative energies are given in kcal/mol and distances in Å

Ion	Basis set	ΔE_s	$r(O_1H_1)$	$r(O_2H_1)$	$\Delta E^{\ddagger}$
Zn^{+2}	3-21G(d, f)	−53.3	1.447	1.060	9.5
	3-21G	−59.4	1.275	1.137	16.6
	Pseudop.	−47.3	1.369	1.037	11.8
	MINI-3	−43.4	1.112	1.329	35.0
Be^{+2}	3-21G(d, f)	−82.8	1.942	0.995	0.1
	3-21G	−84.3	1.708	1.006	0.8
	MINI-3	−53.5	1.183	1.232	22.1
Mg^{+2}	3-21G(d, f)	−47.1	1.346	1.108	14.0
	3-21G	−51.4	1.151	1.255	21.8
	Pseudop.	−42.8	1.381	1.065	19.6
	MINI-3	−37.9	1.080	1.394	51.4

Regarding pseudopotential results, and by comparison with those obtained with all electron 3-21G(d, f) calculations, one can see that they reproduce well the energy profiles and are qualitatively good for geometries. The small differences may arise from the fact that in the pseudopotential basis sets only *d* orbitals are split and no polarization functions are included. In any event, the qualitative conclusions issued from the 3-21G(d, f) basis set results could equally be made from the pseudopotential results.

Another remarkable point is that the MINI-3 results are quite different from those obtained by the other two basis sets. That difference is even larger in the case of Be^{+2}. The MINI-3 basis set has no 2*p* (Be), 3*p* (Mg), or 4*p* (Zn) functions, so it cannot account correctly for the Lewis acid character. It fails thus to describe the proton transfer reaction, due to the importance of empty *p* orbitals along the reaction coordinate. Such failure is more important in Be than in Zn or Mg, because the 3-21G(d, f) basis set shows that Be^{+2} *p* orbitals are very low in energy. It is worth noting that since the MINI-3 basis set does not allow for charge transfer to the metal *p* orbitals, the results obtained are very similar to the dipositive charge results. The aforementioned results show that the MINI-3 basis set must be disregarded for this kind of study, whereas pseudopotentials and 3-21G calculations can be used with some caution. If results from MINI-3 basis set are not considered, the values in Table 8 show that geometries are more sensitive than energetics to the different basis set used.

3.4. Effects of the ligands

So far we have considered only the effect of a naked ion on the proton transfer in the water dimer. Really, the ion will be surrounded by either a first shell of solvation, or (in the carbonic anhydrase) three imidazole groups. To examine the effect of the ligands in this proton transfer we have studied the $(NH_3)_3Zn(H_2O)_2^{+2}$ system. A related complex for which calculations have been

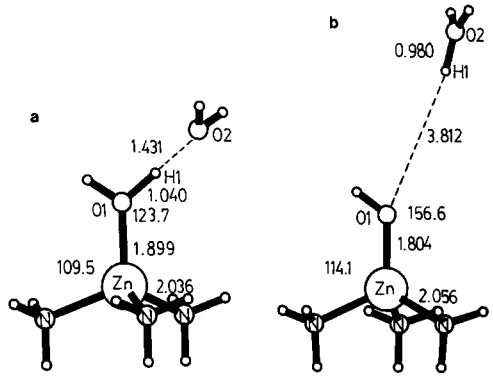

Fig. 6. Optimized structures of (**a**) the hydrogen bond complex and (**b**) the transition state both computed with the 3-21G basis set for the $(NH_3)_3Zn^{+2}(H_2O)_2$ system

carried out previously in $(NH_3)_3Zn(OH)^+$. Using pseudopotentials, Kitchen and Allen [24] found 167 kcal/mol for the proton affinity of this complex. Our best value at the 3-21G(d, f)//3-21G level is 176 kcal/mol, which does not differ much from their result.

The intermediate and the transition state found in this study of the proton transfer in the $(NH_3)_3Zn(H_2O)_2^{+2}$ complex are depicted in Fig. 6. In Table 9 the most important geometrical parameters, charges on the zinc atom and the H_3O group, and relatives energies referred to reactants for the different intervening species are reported.

Comparing the values for the most important geometrical parameters of the $(NH_3)_3Zn(H_2O)_2^{+2}$ and the $Zn(H_2O)_2^{+2}$ intermediates in Tables 1 and 9, one can see that the $Zn-O_1$ bond length has increased when the ligands have been taken into account. This larger $Zn-O_1$ distance should reduce the electrostatic effect noticeably. Further, from the values of the O_1-H_1 and O_2-H_1 bond lengths, and from the values of their Pauling bond orders in the $(NH_3)_3Zn(H_2O)_2^{+2}$ intermediate ($B(O_1-H_1)=0.774$ and $B(O_2-H_1)=0.228$), it can be shown that H_1 is not transferred yet in $(NH_3)_3Zn(H_2O)_2^{+2}$. Further, the intermediate can be seen as $(NH_3)_3Zn(H_2O)^{+2}$ interacting with a water molecule. The TS is now found later along the reaction coordinate, R_c being 2.832 Å for the coordinated zinc, and 1.850 Å for the naked ion. This notwithstanding, the nature of the transition state is similar in both cases, i.e., the H_3O^+ group has been already formed and

Table 9. Distances from O_1 to the metal, distances from oxygens to the transferring hydrogen, charges on the metal (q_M) and H_3O fragment ($q_{(H_3O)}$), and relatives energies referred to reactants computed with the 3-21G (ΔE) and 3-21G(d, f)//3-21G (ΔE_p) for the $(NH_3)_3Zn^{+2}(H_2O)_2$ species. Distances are given in Å, charges in atomic units, and energies in kcal/mol

Species	$r(ZnO_1)$	$r(O_1H_1)$	$r(O_2H_1)$	q_M	$q_{(H_3O)}$	ΔE	ΔE_p
Reactants	1.927	0.949	∞	1.314	—	0.	0.
Intermediate	1.899	1.040	1.431	1.293	0.674	−39.0	−31.8
Transition state	1.804	3.812	0.980	1.167	0.999	17.6	23.2
Products	1.751	∞	0.974	1.193	1.000	−15.5	−6.0

is moving away from the other fragment. This can be also seen from the values of the eigenvector associated to the only negative eigenvalue of the Hessian matrix. The main component of this vector, which corresponds to the $R(O_2-H_1)$ distance has a value of 0.9925, showing that the separation of the H_3O^+ and the $(NH_3)_3Zn(OH)^+$ fragments is the most important component in the transition state.

When ligands are considered, the intermediates are less stabilized referred to reactants, and the energy barrier referred to intermediates increases substantially, now being 55.0 kcal/mol at the 3-21G(d, f)//3-21G level. Further, the reaction becomes less exothermic. Thus, according with the Hammond principle, the intermediate appears earlier and the transition state later along the reaction coordinate. All in all, the presence of the ligands unfavours this proton transfer. These facts will be explained in the following paragraph considering the decrease of both the electrostatic and charge transfer effects due to the presence of the ligands.

From the charges on the metal in Table 9 it can be seen that the ligands transfer an important amount of charge to the central ion. For instance, in the $(NH_3)_3Zn(H_2O)^{+2}$ reactant the charge transfer from the three ammonia ligands computed with the 3-21G basis set is 0.494 electrons. The charge transfer from the ligands to zinc reduces the positive charge about the central ion. Moreover, the *s* and *p* metal orbitals receiving the charge transfer from the water dimer are destabilized by the ligands. The *s* and *p* orbitals are now mixed with the ligand orbitals. The bonding combination corresponds to the previous orbitals of the ligand staying almost unchanged, whereas the antibonding combination corresponds to the initial *s* and *p* metal orbitals which have been destabilized in the process. Thus, both aspects contribute to the decrease of the electrostatic and charge transfer effects. This point is also stressed from a Morokuma decomposition analysis of the $(NH_3)_3Zn(H_2O)_2^{+2}$ intermediate performed at the 3-21G level. In this case, considering the $(NH_3)_3Zn^{+2}$ and $(H_2O)_2$ fragments, the ES + PL and CT terms are -111.9 and -15.8 kcal/mol, respectively, as compared to -241.5 and -33.3 kcal/mol obtained for the $Zn(H_2O)_2^{+2}$ intermediate at the 3-21G(d, f)//3-21G level. Both contributions to the interaction energy are reduced by *ca.* one half.

It is worth noting the large similarity, from both geometrical and energetic points of view, between the results obtained for the $(NH_3)_3Zn(H_2O)_2^{+2}$ system and the case of a dipositive charge placed at 1.9 Å from the water dimer (Table 4). This similarity emerges through compensation of the different terms implied. Nevertheless, this result indicates that results which are qualitatively acceptable are obtained if the $(NH_3)_3Zn^{+2}$ complex is modelled by substitution of the zinc atom by a dipositive charge located in the same position.

Finally, our results show that the energy barrier for the proton transfer in the water dimer catalyzed by a triply coordinated Zn^{+2} is very high (55.0 kcal/mol). The $(NH_3)_3Zn(H_2O)^{+2}$ complex has been used as a model for the active site of Carbonic Anhydrase (CA) enzyme in other theoretical calculations [25]. However, the large value of 55.0 kcal/mol obtained cannot be directly related to the intermolecular proton transfer in CA. In the enzyme the proton transfer necessary to generate the Zn^{+2}-(OH^-) active species takes place through a bridge of two water molecules to the His-64 group, and from this intermediate acceptor to the buffer [2g]. In this case, it is believed that the driving force necessary for this proton transfer is given by the His-64 group, which is a much more basic group than water.

4. Conclusions

We have shown in this paper that dications can catalyze the proton transfer process in the water dimer, giving rise to the MOH^+ species, which is necessary in many biochemical catalytic processes.

The presence of an M^{+2} ($M = Zn, Be, Mg$) cation changes the U-shaped profile of the proton transfer in the $H(H_2O)_2^+$ species, so an unsymmetrical profile appears. It has been shown that the overall process is highly exothermic. A transition state is found corresponding to the separation between the two charged species. The catalytic effect of the metal ions turns out to be the sum of the two effects: electrostatic plus polarization and charge transfer. A Morokuma analysis has shown that among these two effects, the electrostatic plus polarization is the most important one. It is found that the mere presence of a dipositive charge catalyzes the proton transfer, but the charge transfer to the metal is also very important, so dications act also as Lewis acids. It is found that the metal-oxygen distances and the energy differences between the *s* and *p* orbitals of the three studied cations correlate well with the obtained results.

It is shown that Zn^{+2} exhibits intermediate characteristics between Be^{+2} and Mg^{+2}, yet closer to Mg^{+2}. The same order for the metal radical monocations has been previously reported in another catalyzed process [26]. Our results suggest that the catalytic efficiency and specificity of Zn^{+2} arises from an intermediate behaviour, rather than an extreme behaviour. The filled *d* shell of Zn^{+2}, which does not participate directly into bonding, places the empty 4*s* and 4*p* orbitals in the adequate level for an efficient catalysis. It has been shown that *d* orbitals are remarkedly polarizable and cause an important EX term. These two factors have values of the same order resulting in opposite contributions to the interaction energy.

Finally, it has been shown that the charge transfer from the ligands to the zinc dication reduces both the electrostatic and charge transfer effects, thus leading to an increase of the energy barrier and a decrease of the exothermicity of the reaction.

Acknowledgment. This work has been supported by the Spanish "Dirección General de Investigación Científica y Técnica" under Project No. PB86-0529.

References

1. (a) Scheiner S (1985) Acc Chem Res 18:174; (b) Cao HZ, Allavena M, Tapia O, Evleth EM (1985) J Phys Chem 89:1581
2. (a) Sen AC, Tu CK, Thomas H, Wynns GC, Silverman DN (1986) Zinc enzymes, Vol 1, Bertini I, Luchinat C, Maret W, Zeppezauer M (eds) Birkhäuser, Boston, p 329; (b) Silverman DN, Lindskog S (1988) Acc Chem Res 21:30; (c) Rowlett RS, Silverman DN (1982) J Am Chem Soc 104:6737; (d) Woolley P (1975) Nature 258:677; (e) Bertini I, Luchinat C (1983) Acc Chem Res 16:272; (f) Fife TH, Przystas TJ (1983) J Am Chem Soc 108:4631; (g) Pocker Y, Janjić N (1989) J Am Chem Soc 111:731
3. Rode BM (1980) Theor Chim Acta 56:245
4. (a) Del Bene JE, Frisch MJ, Pople JA (1985) J Phys Chem 89:3669; (b) Yamabe S, Minato T, Hirao K (1984) J Chem Phys 80:1576; (c) Scheiner S, Szczęśniak MM, Bigham LD (1983) Int J Quantum Chem 23:739; (d) Del Bene JE (1988) J Phys Chem 92:2874
5. Basch H, Krauss M, Stevens WJ (1985) J Am Chem Soc 107:7267
6. Roothaan CC (1951) Rev Mod Phys 23:69

7. Schlegel HB (1982) J Comp Chem 3:214
8. (a) Broyden CG (1970) Math Comp 24:365; (b) Fletcher R (1970) Comp J 13:317; (c) Goldfarb D (1970) Math Comp 24:23; (d) Shanno DF (1970) Math Comp 24:647
9. Del Bene JE (1987) J Comp Chem 8:810
10. (a) Scheiner S, Bigham LD (1985) J Chem Phys 82:3316; (b) Liang JY, Lipscomb WN (1986) J Am Chem Soc 108:5051; (c) Latajka Z, Scheiner S (1985) Chem Phys 98:59; (d) Hillenbrand EA, Scheiner S (1986) J Am Chem Soc 108:7178; (e) Cybulski SM, Scheiner S (1989) J Am Chem Soc 111:23
11. (a) Binkley JS, Pople JA, Hehre WJ (1980) J Am Chem Soc 102:939; (b) Dobbs KD, Hehre WJ (1987) J Comp Chem 8:861
12. Bauschlicher CW, Jr., Langhoff SR (1986) Chem Phys Lett 126:163
13. Hashimoto K, Yoda N, Iwata S (1987) Chem Phys 116:193
14. (a) Tatewaki H, Huzinaga S (1980) J Comp Chem 1:205; (b) Tatewaki H, Sakai Y, Huzinaga S (1981) J Comp Chem 2:278
15. (a) Wadt WR, Hay PJ (1985) J Chem Phys 82:284; (b) Hay PJ, Wadt WR (1985) J Chem Phys 82:270
16. Ditchfied R, Hehre WJ, Pople JA (1971) J Chem Phys 54:724
17. Frisch MJ, Binkley JS, Schlegel HB, Raghavachari K, Melius CF, Martin RL, Stewart JJP, Bobrowicz FW, Rohlfing CM, Kahn LR, Defrees DF, Seeger R, Whiteside RA, Fox DJ, Fleider EM, Pople JA (1984) GAUSSIAN 86, Carnegie-Mellon Quantum Chemistry Publishing Unit, Pittsburgh, PA, USA
18. Peterson MR, Poirier RA (1981) MONSTERGAUSS, Department of Chemistry, University of Toronto, Ontario, Canada
19. (a) Demoulin D, Pullman A (1978) Theor Chim Acta 49:161; (b) Georgiadis R, Armentrout PB (1988) J Phys Chem 92:7060
20. Scheiner S, Redfern P, Szczęśniak MM, Bigham LD (1985) J Phys Chem 89:262
21. (a) Morokuma K (1977) Acc Chem Res 10:294; (b) Nagase S, Morokuma K (1978) J Am Chem Soc 100:1666
22. Rodweel WR, Random L (1981) J Am Chem Soc 103:2865
23. (a) Paz MD, Leventhal JJ, Friedman L (1969) J Chem Phys 51:3478; (b) Kebarle P, Scarles SK, Zolla A, Scarborough J, Arshadi M (1967) J Am Chem Soc 89:6393; (c) Moet-Ner M, Field FH (1977) J Am Chem Soc 99:998; (d) Kabarle P (1977) Annu Rev Phys Chem 28:445
24. Kitchen DB, Allen LC (1989) J Phys Chem 93:7265
25. (a) Pullman A (1981) Ann NY Acad Sci 367:340; (b) Liang JY, Lipscomb WN (1989) Int J Quantum Chem 36:299; (c) Liang JY, Lipscomb WN (1987) Biochemistry 26:5293; (d) Liang JY, Lipscomb WN (1988) Biochemistry 27:8676; (e) Jacob O, Cardenas R, Tapia O (1990) J Am Chem Soc 112:8692
26. Clark T (1989) J Am Chem Soc 111:761